



Cardiac magnetic resonance T2* mapping in patients with COVID-19 pneumonia is associated with serum ferritin level?

Sercin Ozkok^{1,2} · Hatice Ozge Ciftci³ · Nursen Keles⁴ · Mesut Karatas⁵ · Kemal Emre Can Parsova⁴ · Erkan Kahraman⁴ · Furkan Durak⁶ · Kerem Pekkan⁷ · Cevdet Ugur Kocogullari⁸ · Nurettin Yiyit⁹

Received: 31 October 2022 / Accepted: 14 December 2022 / Published online: 21 December 2022
© The Author(s), under exclusive licence to Springer Nature B.V. 2022

Abstract

The coronavirus disease of 2019 (COVID-19)-related myocardial injury is an increasingly recognized complication and cardiac magnetic resonance imaging (MRI) has become the most commonly used non-invasive imaging technique for myocardial involvement. This study aims to assess myocardial structure by T2*-mapping which is a non-invasive gold-standard imaging tool for the assessment of cardiac iron deposition in patients with COVID-19 pneumonia without significant cardiac symptoms. Twenty-five patients with COVID-19 pneumonia and 20 healthy subjects were prospectively enrolled. Cardiac volume and function parameters, myocardial native-T1, and T2*-mapping were measured. The association of serum ferritin level and myocardial mapping was analyzed. There was no difference in terms of cardiac volume and function parameters. The T2*-mapping values were lower in patients with COVID-19 compared to controls (35.37 [IQR 31.67–41.20] ms vs. 43.98 [IQR 41.97–46.88] ms; $p < 0.0001$), while no significant difference was found in terms of native-T1 mapping value ($p = 0.701$). There was a positive correlation with T2*-mapping and native-T1 mapping values ($r = 0.522$, $p = 0.007$) and negative correlation with serum ferritin values ($r = -0.653$, $p = 0.000$), while no correlation between cardiac native-T1 mapping and serum ferritin level. Negative correlation between serum ferritin level and T2*-mapping values in COVID-19 patients may provide a non-contrast-enhanced alternative to assess tissue structural changes in patients with COVID-19. T2*-mapping may provide a non-contrast-enhanced alternative to assess tissue alterations in patients with COVID-19. Adding T2*-mapping cardiac MRI in patients with myocardial pathologies would improve the revealing of underlying mechanisms. Further in vivo and ex vivo animal or human studies designed with larger patient cohorts should be planned.

Keywords Cardiac magnetic resonance imaging (MRI) · COVID-19 · Myocarditis · Ferritin

✉ Sercin Ozkok
sercinbas2005@gmail.com; sozkok20@ku.edu.tr

¹ Department of Radiology, Acıbadem International Hospital, Istanbul, Turkey

² Department of Biomedical Engineering, Koç University, Istanbul, Turkey

³ Department of Radiology, Dr. İlhan Varank Sancaktepe Training and Research Hospital, Istanbul, Turkey

⁴ Department of Cardiology, Dr. Siyami Ersek Thoracic and Cardiovascular Surgery Training and Research Hospital, University of Health Sciences, Istanbul, Turkey

⁵ Department of Cardiology, Kartal Kosuyolu Yuksek Ihtisas Training and Research Hospital, University of Health Sciences, Istanbul, Turkey

⁶ Department of Cardiology, Sancaktepe Şehit Prof Dr İlhan Varank Training and Research Hospital, University of Health Sciences, Istanbul, Turkey

⁷ Department of Mechanical Engineering, Koç University, Istanbul, Turkey

⁸ Department of Cardiovascular Surgery, Dr. Siyami Ersek Thoracic and Cardiovascular Surgery Training and Research Hospital, University of Health Sciences, Istanbul, Turkey

⁹ Department of Thoracic Surgery, Dr. İlhan Varank Sancaktepe Training and Research Hospital, Istanbul, Turkey

Introduction

The coronavirus disease of 2019 (COVID-19) was first identified in China at the end of the 2019, resulting global pandemic and caused more than 102M cases and 2.2M related death worldwide [1, 2]. COVID-19 has variable clinical manifestations ranging from asymptomatic infection to severe acute respiratory failure, multi-organ dysfunction, and death [3]. COVID-19-related myocardial injury, including myocarditis, myocardial infarction, stress cardiomyopathy, heart failure, arrhythmias, and cardiogenic shock is an increasingly recognized complication seen in 8 to 12% of all patients [4]. COVID-19-related myocardial injury, including myocarditis, myocardial infarction, stress cardiomyopathy, heart failure, arrhythmias, and cardiogenic shock, is an increasingly recognized complication seen in 8 to 12% of all patients. Myocardial injury, including myocarditis, myocardial infarction, stress cardiomyopathy, heart failure, arrhythmias, sepsis-related cardiac injury, and cardiogenic shock, have been reported [5–7]. Several mechanisms have been hypothesized, including a pro-inflammatory state caused by cytokine storm, direct viral invasion of cardiomyocytes, a thromboembolic event caused by a hypercoagulable state, atherosclerotic coronary plaque instability, or rupture has been suggested [8–11].

The imaging of myocardial involvement is challenging due to the heterogeneity of the disease and multi-organ involvement. Endomyocardial biopsy is accepted as the gold-standard technique. However, its application in routine clinical practice is limited because of the periprocedural complications and technical difficulties [12]. Non-invasive imaging modalities provide a safe alternative for diagnosing and managing the treatment. Transthoracic echocardiography is the first-choice imaging technique due to its low cost, easy accessibility, and shorter imaging time [13]. Observer dependant assessment, limited ability in tissue characterization, and acoustic window are the main disadvantages. Cardiac magnetic resonance imaging (MRI) is a widely accepted gold standard non-invasive imaging tool because of its unique capability for non-invasive tissue characterization and mapping, which is recommended by multiple statements and reviews for the diagnosis of myocardial disease [14–17]. Myocardial mapping techniques, including native T1/post-contrast T1 mapping (extracellular volume mapping) for fibrosis, T2 mapping for edema, and late gadolinium enhancement for necrosis or fibrosis are decision-making options for the diagnosis of myocardial inflammation and monitoring response the therapy [18, 19]. Unfortunately, the requirement for gadolinium-based contrast agents which is contraindicated in patients with renal failure and hypersensitivity is the main

limitation of the technique [20]. Relatively long scanning time and requiring the precision of appropriate inversion time are other limitations of contrast-enhanced myocardial mapping and tissue characterization techniques [21]. Thus, an alternative imaging tool to assess myocardial disease without needing gadolinium-based contrast agents would be preferable in patients with multi-organ dysfunction and renal insufficiency.

T2* mapping is the current method of choice for the non-invasive assessment of cardiac iron deposition and the evaluation of the response to the treatment with chelation therapy and recommended imaging tool in practically all clinical guidelines relating to iron overload treatment [22]. For all that, recent studies have focused on T2* mapping for post-revascularization hemorrhage [23, 24], hypertrophic cardiomyopathy [25, 26], or myocardial fibrosis [21]. On the other hand, T2* mapping for non-COVID-19 myocarditis has become an area of great interest [27, 28]. Although several studies have been published about the myocardial T1 mapping in COVID-19 related myocardial injury [29] myocardial T2* mapping in COVID-19 has not been evaluated yet. Therefore, we aimed to assess myocardial T2* values in patients with COVID-19 infection without significant cardiac symptoms. To our knowledge, this is the first study that assessed myocardial T2* mapping in COVID-19.

Materials and methods

This prospective study was approved by the institutional research and ethics committee, and informed consent for cardiac MRI examination was obtained from all patients.

Patient selection

A total of 20 healthy subjects and 25 patients with COVID-19 pneumonia between January 2021 and March 2022 were included in the study. All the individuals in the patient group were within two-to-five weeks of hospitalization and diagnosed with COVID-19 by polymerase chain reaction on a swab test at the administration. All the patients had a moderate pulmonary infection. Exclusion criteria were a history of coronary artery disease, hypertension, diabetes, or myocarditis, claustrophobia, contradictions to the gadolinium contrast, MRI non-compatible implants, pacemakers, and cardiac MRI image quality that was not sufficient for analysis. Healthy control subjects without known cardiovascular disease, chest pain, palpitations, exercise intolerance, or systemic inflammation were included in the study. Patients younger than 18 years old were also excluded from the study. The individuals for the control group were retrospectively selected by review of the cardiac MRI database who previously underwent the cardiac MRI without any prior known

cardiac or inflammatory disease with normal biventricular volume, function, and ECG. We confirmed that the individuals in the control group were negative for COVID-19 and cardiac complaints after vaccination during the examination. We recorded demographic and clinical data, including blood tests and cardiac enzymes, from the hospital health information system.

Cardiovascular imaging and technique

All CMR examinations were performed using a 1.5-Tesla scanner (Explorer; GE healthcare systems, Chicago, IL, USA) with a 32-channel phased-array abdominal coil with electrocardiographic gating. The duration of the examination changes between 30 and 35 s. The weight and height of the patients were recorded before the examination and body surface area was calculated by the Mosteller Formula automatically. No gadolinium-based contrast agents or sedation were used.

All the examinations were performed following our institutional standardized cardiac MRI protocol with the imaging parameters below. After three plane localizers through the thorax were revealed, balanced steady-state free precession (bSSFP) cine images for two-chambers, four-chambers, and short axis plane covering the entire ventricles. The parameters of the bSSFP sequence were revealed with the following typical parameters: echo time; 1.4 ms, repetition time; 37.7 ms, bandwidth; 780 Hz/pixel, pixel size; 2.2×2.2 mm, a field of view; 350×350 mm, matrix; 192×146 , flip angle; 55° , slice thickness; 8 mm, and slice gap; 2 mm. The images were acquired during one or two breath-hold of 7 to 13 s duration, depending on the heart rate during the end-expiratory breath hold.

Native-T1 map and T2* sequences were performed in 3 short axis slices at the basal, mid, and apical short axis at the same imaging plane using a breath-held. Native-T1 mapping was acquired using an electrocardiograph-triggered single-shot modified Look-Locker inversion recovery (MOLLI) sequence during diastole using a 5(3)3 sequence. The acquisition parameters were: echo time; 1.5 ms, repetition time; 3.8 ms, bandwidth; 1250 Hz/pixel, pixel size; 2.2×2.2 mm, field of view; 320×360 mm, matrix; 192×144 , flip angle; 35° , slice thickness; 8 mm, and acceleration factor; 2. The T2* mapping was acquired using a multi-TE gradient echo with different TE times; 3, 7, 10, 14, 17, 20, 23, 26, and 29 ms, TR; 13.2 ms, flip-angle; 20° , bandwidth; ± 83.33 kHz, matrix; 128×256 , FOV; 350×350 mm, NEX; 1, slice thickness; 8 mm.

All the cardiac MRI analyses were performed using Circle cvi42 software (Circle Cardiovascular Imaging, Calgary, Canada) by ten years experienced radiologist (trained in cardiac MRI with an experience with more than 800 cardiac MRI examinations). The endocardial layer of both

ventricles was contoured manually on short-axis cine images by including the papillary muscles and the trabeculations through all slices on end-diastolic and end-systolic phases to calculate ventricular volume and function. Ejection fraction, indexed end-diastolic and end-systolic volumes (EDV and ESV, respectively) were calculated automatically. Native-T1 and T2* mappings were traced in the respective Cvi42 modules (Fig. 1). Endocardial and epicardial borders of the left ventricle were traced manually at the same 3 imaging planes in base, middle, and apical segments of left ventricle. Pericardial fat tissue and ventricular blood pool were not included in ROI measurements to avoid partial volume averaging artifacts at the same imaging plane.

Statistics

The analysis of the obtained data was assessed with SPSS version 20.0 software (IBM Corporation, Armonk, NY, USA). The data were expressed as the mean \pm standard deviation (for normal distribution) or medians and interquartile ranges [IQR] (for non-normal distribution). The Shapiro–Wilk normality test was used to evaluate the normality of the obtained data. The Student's T-test was used to compare the T2* mapping values and other variables between groups. Pearson correlation coefficient (r) for normal distribution data and Spearman correlation coefficient (rho) for abnormal data distribution was performed to evaluate of correlation between cardiac MRI mapping values and serum parameters. $p < 0.05$ was considered statistically significant for all the comparisons.

Results

Twenty-five patients with COVID-19 (14 females and 11 males, mean age of 41.76 ± 10.19 years, median age: 40 years, [IQR 35–49 years] and 20 healthy individuals (9 females and 11 males, mean age of 42.10 ± 9.16 years, median age: 44 years [IQR 35–49 years]) were included to the study ($p = 0.908$). There was no statistically significant difference between the patient and control groups in terms of gender ($p = 0.65$) or body surface area (patient body surface area $1.92 \pm 0.23 \text{ m}^2$ vs. control body surface area $1.99 \pm 0.22 \text{ m}^2$, $p = 0.299$). The laboratory findings of patients with reference values are presented in Table 1. Concerning cardiac MRI assessment, there was no difference between patient and control groups in terms of left ventricular ejection fraction (55.72 [IQR 51.54–59.05% vs. 56.02 [IQR 52.22–59.53] %; $p = 0.712$), left ventricular end-diastolic volume index (74.54 [IQR 61.99–86.32] ml/m^2 vs. 55.15 [IQR 69.67–87.16] ml/m^2 ; $p = 0.536$), right ventricular ejection fraction (52.12 [IQR 46.48–56.77] % vs. 53.11 [IQR

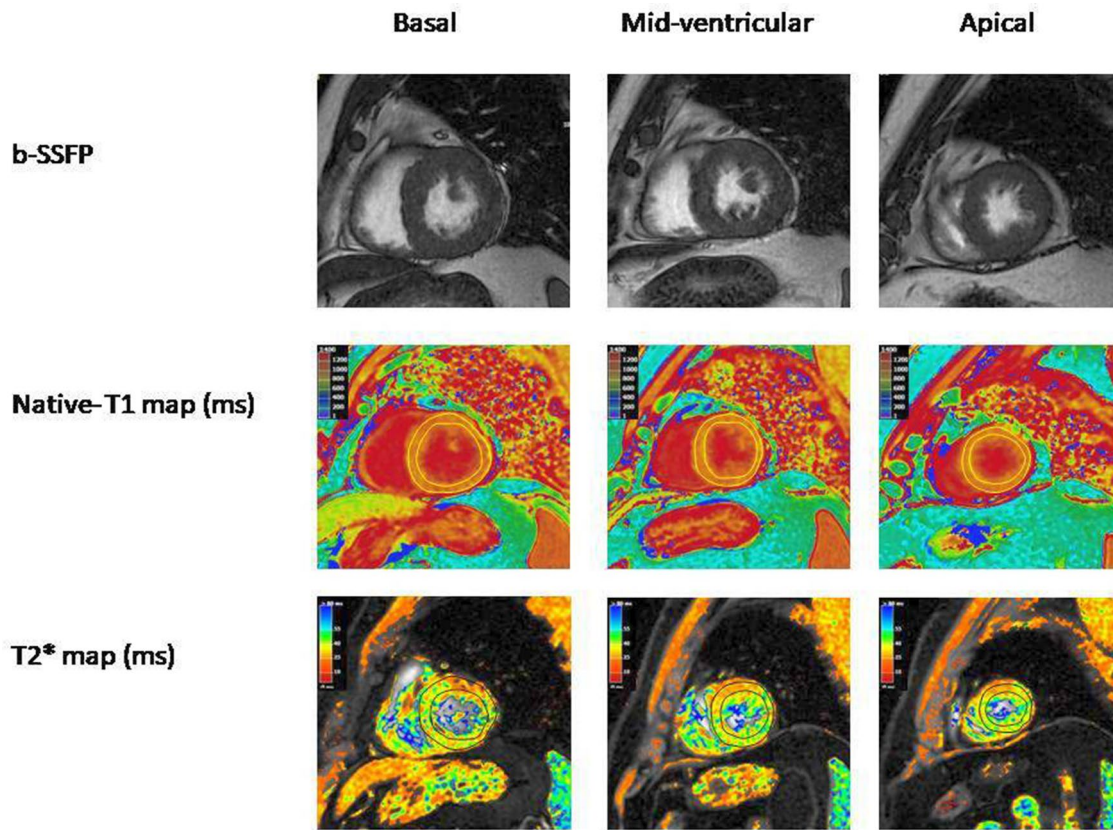


Fig. 1 Multiparametric cardiac magnetic resonance imaging in a 47-year-old male patient with COVID-19. The same slices of short axis view on basal, mid-ventricular, and apical segments (left-to-

right) for b-SSFP, native-T1, and T2* mapping images. Native-T1 and T2* mapping values were calculated for the entire ventricle as 1028 ± 8 ms and 41 ± 6 ms, respectively

Table 1 Serum biochemical characteristics of the patients with COVID-19 and control groups

Serum biochemical characteristics	Reference range	Patient group (n = 25)
Ferritin ($\mu\text{g/l}$)	24–336	616.32 ± 361.14
Troponin I (ng/ml)	0–0.04	1.02 ± 0.829
D-dimer (ng/dl)	0–0.50	0.69 ± 0.83
Hemoglobin (g/dl)	14.00–17.50	12.97 ± 1.67
Haematocrit (%)	41–50	38.95 ± 4.94
Red blood cell $\times 10^9/\text{l}$	4.65–5.45	4.51 ± 0.56
White blood cell $\times 10^9/\text{l}$	4.5–11.0	8.38 ± 2.96
Blood urea nitrogen (mg/dl)	6–24	24.75 ± 7.76
C-reactive protein (mg/l)	0–10	141.48 ± 74.98
Creatinine (mg/dl)	0.65–1.25	0.76 ± 0.18
Low density lipoprotein (mg/dl)	100–129	122.17 ± 31.61
Aspartate aminotransferase (U/l)	8–33	29.22 ± 26.26
Lactate dehydrogenase (IU/l)	105–333	243.14 ± 84.19

Numbers are given as median (25th and 75th percentile interquartile ranges) or mean \pm standard deviation median value

48.16–58.17] %; $p = 0.796$), and right ventricular end-diastolic volume index (68.05 [IQR 60.71 – 80.57] ml/m^2 vs. 73.96 [IQR 66.10 – 81.55] ml/m^2 ; $p = 0.293$). T2*

mapping values were lower in patients with COVID-19 compared to healthy controls (35.37 [IQR 31.67 – 41.20] ms vs. 43.98 [IQR 41.97 – 46.88] ms; $p < 0.0001$), while

there was no significant difference in terms of native-T1 mapping values (1088.02 ms [IQR 1042.83–1140.83 ms] vs. 1073.07 ms [IQR 1044.37–1098.01 ms]; $p=0.701$). Cardiac MRI parameters of both groups are presented in Table 2.

There was a positive correlation with T2* mapping and native-T1 mapping values ($r=0.522$, $p=0.007$) and negative correlation with serum ferritin values ($r=-0.653$, $p=0.000$) (Fig. 2) (Table 3). However, there was no correlation between cardiac T2* mapping and serum troponin-I, d-dimer values ($r=0.434$, $p=0.056$ and $r=0.092$, $p=0.692$, respectively) (Table 3). There was no correlation between cardiac native-T1 mapping and serum ferritin, troponin, d-dimer values ($r=-0.151$, $p=0.470$, $r=0.043$, $p=0.857$, and $r=-0.089$, $p=0.700$, respectively) (Fig. 3) (Table 3).

Discussion

In this study, the T2* mapping value was found to be significantly higher in patients with COVID-19 compared to healthy subjects. However, no significant difference was found between two groups in terms of native-T1 mapping value. There was a significantly negative correlation between T2* mapping and serum ferritin level in patients with COVID-19 infection and a positive correlation between T2* and native-T1 mapping values. However, no significant correlation was found between the native-T1 mapping value and serum ferritin level.

T2* mapping is able to characterize the relaxation of the transverse magnetization that is influenced by magnetic field inhomogeneities composed of two elements. One is spin–spin interaction effect that is caused by its own

Table 2 Cardiac MRI characteristics of the patients with COVID-19 and control groups

Cardiac MRI characteristics	Patient group (n=25)	Control group (n=20)	P-value
LV- ejection fraction (%)	55.72 (51.54–59.05)	56.02 (52.22–59.53)	0.712
LV-EDVI (ml/m ²)	74.54 (61.99–86.32)	55.15 (69.67–87.16)	0.536
LV-ESVI (ml/m ²)	31.19 (27.18–40.34)	33.75 (30.84–37.48)	0.772
LV-SVI (ml/m ²)	39.68 (31.97–49.60)	41.26 (35.15–53.07)	0.459
RV- ejection fraction (%)	52.12 (46.48–56.77)	53.11 (48.16–58.17)	0.796
RV-EDVI (ml/m ²)	68.05 (60.71–80.57)	73.96 (66.10–81.55)	0.293
RV-ESVI (ml/m ²)	34.69 (27.88–41.08)	34.59 (29.58–42.18)	0.621
RV-SVI (ml/m ²)	35.35 (30.60–45.44)	38.41 (32.33–45.32)	0.611
Myocardial native T1 map value (entire ventricle, ms)	1088.02 (1042.83–1140.83)	1073.07 (1044.37–1098.01)	0.701
Myocardial T2* map value (entire ventricle, ms)	35.37 (31.67–41.20)	43.98 (41.97–46.88)	<0.0001

Numbers are given as median (25th and 75th percentile interquartile ranges) or mean ± standard deviation median value. p; p-value of independent samples Student’s t tests. p value is significant if <0.05

MRI magnetic resonance imaging, RV right ventricle, LV left ventricle, EDVI end-diastolic volume index, ESVI end-systolic volume index, SVI stroke volume index

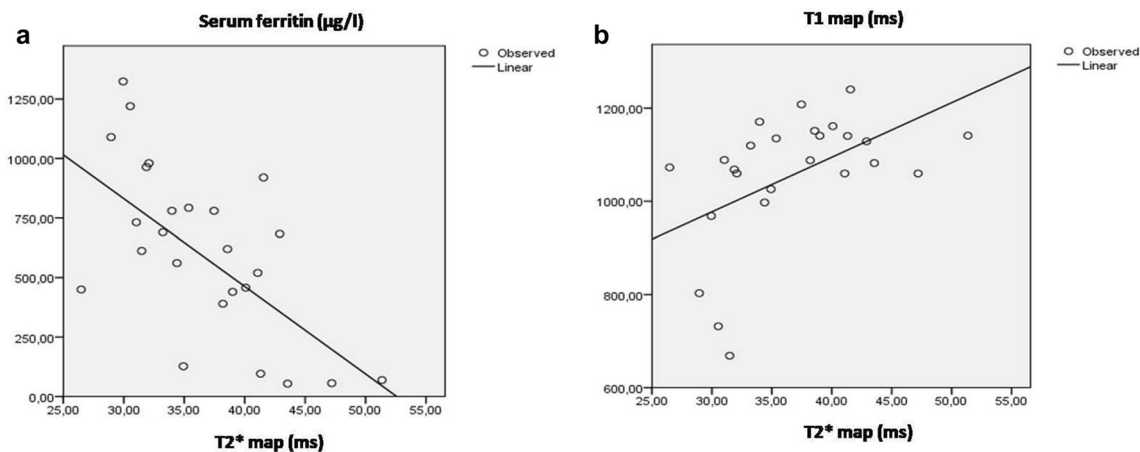


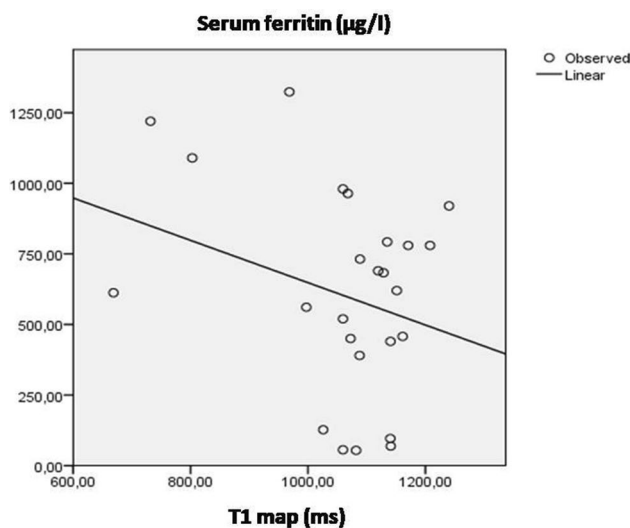
Fig. 2 Correlation of mean T2* mapping value with serum ferritin (a, left) and native-T1 mapping (b, right) values

Table 3 Correlation between serum parameters with myocardial native-T1 map and T2* map values

	Native-T1 map	Ferritin	Troponin-I	D-dimer
T2* map				
r	0.522	− 0.653	0.434	0.092
p	0.007 ^b	0.000 ^a	0.056 ^b	0.692 ^b
Native-T1 map				
r	−	− 0.151	0.043	− 0.089
p	−	0.470 ^b	0.857 ^b	0.700 ^b
Ferritin				
r	−	−	− 0.382	− 0.259
p	−	−	0.096 ^b	0.257 ^b
Troponin-I				
r	−	−	−	0.317
p	−	−	−	0.187 ^b

^aPearson's correlation test

^bSpearman's correlation test. p;p value of correlation test, r; correlation coefficient, p value is significant if <0.05

**Fig. 3** Correlation between mean native-T1 mapping value with serum ferritin

inhomogeneities, terms as a macroscopic effect. The second one is the local magnetic field susceptibility changes caused by the structure of the tissue as a mesoscopic effect [15, 30]. Thus, the T2* relaxation time is a more sensitive measure to evaluate the structural and pathological changes in tissue [24]. T2* mapping assessment of microvascular obstruction, acute myocardial infarction, and intramyocardial hemorrhage [23, 24, 31] has become of great interest in recent years. Hemoglobin aggregation within infarcted areas of the myocardium causes signal nulling [31]. Iron shortens T2* relaxation times and can be measured by T2* mapping[32].

The exact mechanisms of myocardial injury in COVID-19 have not been completely understood. Most likely mechanisms are suggested to be direct virus-mediated cytotoxicity, dysregulation of the renin–angiotensin–aldosterone system, endothelial cell damage, thrombo-inflammation, dysregulation of the immune response, and hypoxic injury [12]. It is suggested that the endothelium has a crucial role in the pathogenesis of severe COVID-19, inducing both pro-coagulant and inflammatory responses [33, 34]. In addition to the direct cytopathic viral effect, severe COVID-19 infection would involve both large and microscopic blood vessels. It can be complicated by infection-induced microangiopathy or thromboembolic disease that causes capillary, venous and/or arterial thrombosis and end-organ damage [35]. It is also mentioned that microthrombi is to be associated with myocyte necrosis in autopsy studies [36]. Additional several ischemic mechanisms, including type-2 myocardial infarction and non-ischemic mechanisms, such as microangiopathic thrombosis, have also been proposed to be responsible [37]. Considering the possibility of hemorrhages, thrombi, or dysregulation of iron metabolism, we hypothesized that measurement of iron deposition through myocardial T2* mapping without using contrast agents injection could be used to assess myocardial changes in patients with COVID-19.

T2* mapping for non-COVID-19 myocarditis has been assessed in two MRI studies [27, 28]. Helluy et al. [27] assessed myocardial injury in murine models of acute and chronic viral myocarditis by T2* mapping [27]. Although quantitative assessment has not been performed and T2* mapping values not computed, direct localization of virus-induced myocardial lesions ex vivo and in vivo was demonstrated by T2* imaging without any MRI tracer or contrast agent [27]. It is also mentioned that T2* mapping has the capability to detect both small cardiac lesions of acute myocarditis and larger necrotic areas at later stages of chronic myocarditis, which was correlated histopathologically [27]. In another study by Baxan et al. [28] assessed acute hemorrhagic myocarditis in ex vivo histopathologic correlation with in vivo cardiac MRI using T2* sequence in the animal model and suggested that low T2* detecting areas of increased levels of iron in the tissue suggestive of inflammatory changes including vascular damage, red blood cell extravasation, and tissue iron deposition.

Hyperferritinemia in patients with COVID-19 infection and the association of high ferritin levels with the severity of the illness and mortality have been investigated early in the course of the pandemic [38]. Dysregulated iron metabolism is suggested to be responsible in severe COVID-19 disease [38, 39]. Although the exact mechanisms of ferroptosis and the association between iron are not clearly identified yet, it is well known the crucial role of iron metabolism in ferroptosis, which is a recently identified type of controlled cell

death leading to excessive reactive oxygen species formation, lipid peroxidation triggered by intracellular iron accumulation, decreased iron storage capacity and glutathione depletion [39, 40].

In addition to reducing the need for myocardial biopsy, *in vivo* and *ex vivo* experiments have made significant advances in cardiac MRI, which is now considered the clinical gold standard for non-invasive detection of myocardial damage and structural changes. Researches about COVID-19 and its cardiac effects have recently focused on *in vitro* and *ex vivo* studies [39, 41]. An *in vivo* study by Sharma et al. [41] demonstrated that COVID-19 could infect and induce apoptosis in human induced pluripotent stem cell-derived cardiomyocytes. Although ferroptosis is not investigated in this study, it is an essential point that myocarditis is caused by a direct viral infection instead of immune cell infiltration. In another study by Baier et al. [39], iron metabolism and association with ferroptosis were investigated in the left ventricular myocardium of patients who had died due to severe COVID-19. They found that increased intracellular iron concentration is associated with the inhibition of detoxifying enzymes (GPX4) as well as activation of the ferroptosis pathway (HMOX-1), leading to increased myocardial oxidative stress with subsequent myocardial damage. Although a direct relationship between cardiac iron overload and cardiac injury in COVID-19 infection was shown, the study lacks cardiac imaging and clinical correlation to corroborate the postmortem findings. Dysregulation of iron metabolism and its role in neurological, renal, circulatory, and immune system regulation is also implicated [39]. This multisystem involvement would explain the heterogeneous clinical symptoms and multiple organ involvement in COVID-19.

Another study by Han Y. et al. has defined that sinoatrial pacemaker cells are infected directly by the COVID-19 virus and induced ferroptosis [42]. Another important finding of this study is that the treatment of deferoxamine which is used as a chelator of iron overload and known to be an inhibitor of ferroptosis, blocked the viral entry of COVID-19 and inhibited ferroptosis. The effect of iron chelators is seen in multiple steps, such as chelating iron, inhibiting redox properties exerted by free iron, and hindering the participation of iron in Fenton reactions which allows inhibition of hydroxyl radical production as well as the creation of other ROS that protect oxidative stress and ferroptosis [43]. It is also shown that iron chelators block ferroptotic cell death *in vitro* and *in vivo* [43]. Iron chelators have been used to treat cytokine storms and multi-organ injuries in a variety of environments, including ischemia–reperfusion injury, sepsis, and infections, and have been shown to help with several viral infections, including HIV-1, hepatitis B, and mengovirus infection, among others [44]. Prospective studies in human and animal models are needed to fully elucidate the efficacy and safety of iron-chelating agents in the therapeutic

armamentarium of COVID-19, probably as an adjunctive treatment.

Our result (negative correlation between cardiac T2* mapping and serum ferritin) indicates that increased ferritin level would decrease myocardial T2* mapping values in COVID-19. We suggest that a negative correlation between myocardial T2* mapping value and ferritin level would be suggestive of microhemorrhages in the macroscale aspect or ferroptosis-mediated myocardial cell destruction in the microscale aspect. Although it is known that iron shortens both T1 and T2* relaxation times [32], no significant difference was found between the control and patient groups in terms of native-T1 mapping in our study. Recent studies have demonstrated that T1 mapping with prolonged T1 relaxation time is a useful diagnostic tool in the assessment of fibrosis and interstitial remodeling of the myocardium [45]. However, the current evidence conflicts with recent studies reporting decreased T2* values in hypertrophic cardiomyopathy [26, 46] or in post-myocardial infarction [21], especially those who had myocardial fibrosis or fibrotic segments. The result of our study with decreased T2* value without increased native-T1 value is speculative. Regarding this finding, we hypothesize that potential discrepancies in oxygen delivery to the myocardial tissue or a complex interaction between fibrosis and myocardial inflammation might be involved. It is suggested that reduced T2* mapping values in patients with hypertrophic cardiomyopathy are potentially triggered by relative ischemia [21]. Another hypothesis is that decreased levels of oxyhemoglobin and oxymyoglobin in case of reduced perfusion may be associated with reduced T2* values because of the paramagnetic effect of deoxygenated proteins [46]. On the other hand, reduced T1 mapping value is reported at follow-up examinations 68 days after the baseline scan [47]. Depending on the severity of the microhemorrhage or hypoperfusion and the regional/segmentary or diffuse involvement, there might be either an improper immune response with persistent inflammation [16, 47] or a more subtle and diffuse process that drives the changes after COVID-19. Concerning the correlation between cardiac MRI measurements and serum parameters, there was no correlation between cardiac MRI mapping and serum troponin-I, d-dimer values. Previous studies have shown that high troponin levels are associated with increased mortality in patients with COVID-19. However, abnormal troponin levels are not necessarily a sign of an acute course of myocarditis [4].

The current study has a number of limitations. First, the study cohort is limited. A multicenter study with a larger patient group would strengthen the results. Second, the absence of late gadolinium-enhanced imaging or CMR perfusion imaging and verifying the relation between T2* and fibrosis. However, studies from different tissues have already shown the value of native-T1 mapping for detecting

fibrosis [24]. Cardiac MRI also has its limitations, such as higher cost, longer scanning time, and the need for trained specialists.

In conclusion, the negative correlation between serum ferritin level and T2* mapping values in COVID-19 patients may provide a non-contrast-enhanced alternative to assess tissue structural changes in patients with COVID-19. Adding T2 * cardiac MRI mapping in patients with myocardial pathologies would improve reveal underlying mechanisms without contrast agent injection. In vivo and ex vivo animal or human studies designed with larger patient cohorts and correlation with histopathological findings should be planned in the future.

Author contributions Study conception and design SO. Material preparation, data collection and analysis were performed by SO and HOC. The first draft of the manuscript was written by SO and all authors commented on previous versions of the manuscript. All authors read and approved the final manuscript.

Funding The authors declare that no funds, Grants, or other support were received during the preparation of this manuscript.

Declarations

Competing interests The authors have no relevant financial or non-financial interests to disclose.

Ethical approval All procedures performed in studies involving human participants were in accordance with the ethical standards of the institutional and/or national research committee and with the 1964 Helsinki declaration and its later amendments or comparable ethical standards. This article does not contain any studies with human participants or animals performed by any of the authors.

Consent to participate Written informed consent was obtained from all individual participants included in the study.

Consent to publish The authors affirm that human research participants provided informed consent for publication of the images in Figs. 1, 2a, b and 3.

References

- World Health Organization (2020) Coronavirus disease 2019 (COVID-19) situation report-51. Available at: <https://www.who.int/docs/default-source/coronaviruse/situation-reports/20200311-sitrep-51-covid-19.pdf>. Accessed 28 Jan 2021
- World Health Organization (2021) Actualización epidemiológica semanal COVID-19. World Health Organization, pp 1–3
- Chakurkar V, Rajapurkar M, Lele S et al (2021) Increased serum catalytic iron may mediate tissue injury and death in patients with COVID-19. *Sci Rep* 11(1):19618. <https://doi.org/10.1038/s41598-021-99142-x>
- Paramasivam A, Priyadharsini JV, Raghunandhakumar S, Elumalai P (2020) A novel COVID-19 and its effects on cardiovascular disease. *Hypertens Res* 43(7):729–730. <https://doi.org/10.1038/s41440-020-0461-x>
- Chen T, Wu D, Chen H, Yan W, Yang D, Chen G, Ma K, Xu D, Yu H, Wang H, Wang T, Guo W, Chen J, Ding C, Zhang X, Huang J, Han M, Li S, Luo X, Zhao J, Ning Q (2020) Clinical characteristics of 113 deceased patients with coronavirus disease 2019: retrospective study. *BMJ* 26(368):m1091. <https://doi.org/10.1136/bmj.m1091>. (Erratum in: *BMJ*. 2020 Mar 31;368:m1295)
- Siripanthong B, Nazarian S, Muser D, Deo R, Santangeli P, Khanji MY, Cooper LT Jr, Chahal CAA (2020) Recognizing COVID-19-related myocarditis: the possible pathophysiology and proposed guideline for diagnosis and management. *Heart Rhythm* 17(9):1463–1471. <https://doi.org/10.1016/j.hrthm.2020.05.001>
- Chilazi M, Duffy EY, Thakkar A, Michos ED (2021) COVID and cardiovascular disease: what we know in 2021. *Curr Atheroscler Rep* 23(7):37. <https://doi.org/10.1007/s11883-021-00935-2>
- Kunal S, Madan M, Tarke C, Gautam DK, Kinkar JS, Gupta K, Agarwal R, Mittal S, Sharma SM (2022) Emerging spectrum of post-COVID-19 syndrome. *Postgrad Med J* 98(1162):633–643. <https://doi.org/10.1136/postgradmedj-2020-139585>
- Lee CCE, Ali K, Connell D, Mordi IR, George J, Lang EM, Lang CC (2021) COVID-19-associated cardiovascular complications. *Diseases* 9(3):47. <https://doi.org/10.3390/diseases9030047>
- Martínez-Salazar B, Holwerda M, Stüdle C, Piragyte I, Mercader N, Engelhardt B, Rieben R, Döring Y (2022) COVID-19 and the vasculature: current aspects and long-term consequences. *Front Cell Dev Biol* 10:824851. <https://doi.org/10.3389/fcell.2022.824851>
- Cordeanu EM, Duthil N, Severac F, Lambach H, Toussef J, Lambert L, Mirea C, Delatte A, Younes W, Frantz AS, Merdji H, Schini-Kerth V, Bilbault P, Ohlmann P, Andres E, Stephan D (2020) Prognostic value of troponin elevation in COVID-19 hospitalized patients. *J Clin Med* 9(12):4078. <https://doi.org/10.3390/jcm9124078>
- Nakou E, De Garate E, Liang K, Williams M, Pennell DJ, Bucciarelli-Ducci C (2022) Imaging findings of COVID-19-related cardiovascular complications. *Card Electrophysiol Clin* 14(1):79–93. <https://doi.org/10.1016/j.ccep.2021.10.008>
- Friedrich MG, Sechtem U, Schulz-Menger J, Holmvang G, Alakija P, Cooper LT, White JA, Abdel-Aty H, Gutberlet M, Prasad S, Aletas A, Laissy JP, Paterson I, Filipchuk NG, Kumar A, Pauschinger M, Liu P (2009) International consensus group on cardiovascular magnetic resonance in myocarditis. Cardiovascular magnetic resonance in myocarditis: a JACC white paper. *J Am Coll Cardiol* 53(17):1475–1487. <https://doi.org/10.1016/j.jacc.2009.02.007>
- Kelle S, Bucciarelli-Ducci C, Judd RM, Kwong RY, Simonetti O, Plein S, Raimondi F, Weinsaft JW, Wong TC, Carr J (2020) Society for cardiovascular magnetic resonance (SCMR) recommended CMR protocols for scanning patients with active or convalescent phase COVID-19 infection. *J Cardiovasc Magn Reson* 22(1):61. <https://doi.org/10.1186/s12968-020-00656-6>
- Messroghli DR, Moon JC, Ferreira VM, Grosse-Wortmann L, He T, Kellman P, Mascherbauer J, Nezafat R, Salerno M, Schelbert EB, Taylor AJ, Thompson R, Ugander M, van Heeswijk RB, Friedrich MG (2017) Clinical recommendations for cardiovascular magnetic resonance mapping of T1, T2, T2* and extracellular volume: a consensus statement by the Society for cardiovascular magnetic resonance (SCMR) endorsed by the European association for cardiovascular imaging (EACVI). *J Cardiovasc Magn Reson* 19(1):75. <https://doi.org/10.1186/s12968-017-0389-8>. (Erratum in: *J Cardiovasc Magn Reson*. 2018;20(1):9)
- Puntmann VO, Carerj ML, Wieters I, Fahim M, Arendt C, Hoffmann J et al (2020) Outcomes of cardiovascular magnetic resonance imaging in patients recently recovered from coronavirus disease 2019 (COVID-19). *JAMA Cardiol* 5(11):1265–1273. <https://doi.org/10.1001/jamacardio.2020.3557>
- Goerlich E, Minhas AS, Mukherjee M, Sheikh FH, Gilotra NA, Sharma G et al (2021) Multimodality imaging for cardiac

- evaluation in patients with COVID-19. *Curr Cardiol Rep* 23(5):44. <https://doi.org/10.1007/s11886-021-01483-6>
18. Ferreira VM, Schulz-Menger J, Holmvang G, Kramer CM, Carbone I, Sechtem U, Kindermann I, Gutberlet M, Cooper LT, Liu P, Friedrich MG (2018) Cardiovascular magnetic resonance in nonischemic myocardial inflammation: expert recommendations. *J Am Coll Cardiol* 72(24):3158–3176. <https://doi.org/10.1016/j.jacc.2018.09.072>
 19. Liguori C, Farina D, Vaccher F, Ferrandino G, Bellini D, Carbone I (2020) Myocarditis: imaging up to date. *Radiol Med* 125(11):1124–1134. <https://doi.org/10.1007/s11547-020-01279-8>
 20. Perazella MA (2008) Gadolinium-contrast toxicity in patients with kidney disease: nephrotoxicity and nephrogenic systemic fibrosis. *Curr Drug Saf* 3(1):67–75. <https://doi.org/10.2174/157488608783333989>
 21. van Nierop BJ, Bax NA, Nelissen JL, Arslan F, Motaal AG, de Graaf L, Zwanenburg JJ, Luijten PR, Nicolay K, Strijkers GJ (2015) Assessment of myocardial fibrosis in mice using a T2*-weighted 3D radial magnetic resonance imaging sequence. *PLoS ONE* 10(6):e0129899. <https://doi.org/10.1371/journal.pone.0129899>
 22. Angelucci E, Barosi G, Camaschella C, Cappellini MD, Cazzola M, Galanello R, Marchetti M, Piga A, Tura S (2008) Italian Society of Hematology practice guidelines for the management of iron overload in thalassemia major and related disorders. *Haematologica* 93(5):741–752. <https://doi.org/10.3324/haematol.12413>
 23. Kali A, Tang RL, Kumar A, Min JK, Dharmakumar R (2013) Detection of acute reperfusion myocardial hemorrhage with cardiac MR imaging: T2 versus T2. *Radiology* 269(2):387–395. <https://doi.org/10.1148/radiology.13122397>
 24. Mohammadzadeh A, Maleki Z, Nahardani A, Mohammadzadeh M (2018) Correlations of T2* mapping with delayed gadolinium enhancement in chronic myocardial infarction magnetic resonance imaging. *Iran J Radiol* 15(4):e12688. <https://doi.org/10.5812/iranjradiol.12688>
 25. Gastl M, Gruner C, Labucay K, Gotschy A, Von Spiczak J, Polacin M, Boenner F, Kelm M, Ruschitzka F, Alkadhi H, Kozerke S, Manka R (2020) Cardiovascular magnetic resonance T2* mapping for the assessment of cardiovascular events in hypertrophic cardiomyopathy. *Open Heart* 7(1):e001152. <https://doi.org/10.1136/openhrt-2019-001152>
 26. Gastl M, Gotschy A, von Spiczak J, Polacin M, Bönner F, Gruner C, Kelm M, Ruschitzka F, Alkadhi H, Kozerke S, Manka R (2019) Cardiovascular magnetic resonance T2* mapping for structural alterations in hypertrophic cardiomyopathy. *Eur J Radiol Open* 4(6):78–84. <https://doi.org/10.1016/j.ejro.2019.01.007>. **(Erratum in: Eur J Radiol Open. 2020 Dec 17;8:100308)**
 27. Helluy X, Sauter M, Ye YX, Lykowsky G, Kreutner J, Yilmaz A, Jahns R, Boivin V, Kandolf R, Jakob PM, Hiller KH, Klingel K (2017) In vivo T2* weighted MRI visualizes cardiac lesions in murine models of acute and chronic viral myocarditis. *PLoS ONE* 12(3):e0172084. <https://doi.org/10.1371/journal.pone.0172084>
 28. Baxan N, Papanikolaou A, Salles-Crawley I, Lota A, Chowdhury R, Dubois O, Branca J, Hasham MG, Rosenthal N, Prasad SK, Zhao L, Harding SE, Sattler S (2019) Characterization of acute TLR-7 agonist-induced hemorrhagic myocarditis in mice by multiparametric quantitative cardiac magnetic resonance imaging. *Dis Model Mech* 12(8):dmm040725. <https://doi.org/10.1242/dmm.040725>
 29. Santoso A, Pranata R, Wibowo A, Al-Farabi MJ, Huang I, Antariksa B (2021) Cardiac injury is associated with mortality and critically ill pneumonia in COVID-19: a meta-analysis. *Am J Emerg Med* 44:352–357. <https://doi.org/10.1016/j.ajem.2020.04.052>
 30. van Oorschot JW, Gho JM, van Hout GP, Froeling M, Jansen Of Lorkeers SJ, Hoefler IE, Doevendans PA, Luijten PR, Chamuleau SA, Zwanenburg JJ (2015) Endogenous contrast MRI of cardiac fibrosis: beyond late gadolinium enhancement. *J Magn Reson Imaging* 41(5):1181–1189. <https://doi.org/10.1002/jmri.24715>
 31. Menacho K, Abdel-Gadir A, Moon JC, Fernandes JL (2019) T2* mapping techniques: iron overload assessment and other potential clinical applications. *Magn Reson Imaging Clin N Am* 27(3):439–451. <https://doi.org/10.1016/j.mric.2019.04.008>
 32. Wood JC, Otto-Duessel M, Aguilar M, Nick H, Nelson MD, Coates TD, Pollack H, Moats R (2005) Cardiac iron determines cardiac T2*, T2, and T1 in the gerbil model of iron cardiomyopathy. *Circulation* 112(4):535–543. <https://doi.org/10.1161/CIRCULATIONAHA.104.504415>
 33. Lowenstein CJ, Solomon SD (2020) Severe COVID-19 is a microvascular disease. *Circulation* 142(17):1609–1611. <https://doi.org/10.1161/CIRCULATIONAHA.120.050354>
 34. Ince C, Mayeux PR, Nguyen T, Gomez H, Kellum JA, Ospina-Tascón GA, Hernandez G, Murray P, De Backer D, ADQI XIV Workgroup (2016) The endothelium in sepsis. *Shock* 45(3):259–270. <https://doi.org/10.1097/SHK.0000000000000473>
 35. Bilaloglu S, Aphinyanaphongs Y, Jones S, Iturrate E, Hochman J, Berger JS (2020) Thrombosis in hospitalized patients with COVID-19 in a New York City health system. *JAMA* 324(8):799–801. <https://doi.org/10.1001/jama.2020.13372>
 36. Pellegrini D, Kawakami R, Guagliumi G, Sakamoto A, Kawai K, Gianatti A, Nasr A, Kutys R, Guo L, Cornelissen A, Faggi L, Mori M, Sato Y, Pescetelli I, Brivio M, Romero M, Virmani R, Finn AV (2021) Microthrombi as a major cause of cardiac injury in COVID-19: a pathologic study. *Circulation* 143(10):1031–1042. <https://doi.org/10.1161/CIRCULATIONAHA.120.051828>
 37. Montone RA, Iannaccone G, Meucci MC, Gurgoglione F, Niccoli G (2020) Myocardial and microvascular injury due to coronavirus disease 2019. *Eur Cardiol* 15:e52. <https://doi.org/10.15420/ecr.2020.22>
 38. Cheng L, Li H, Li L, Liu C, Yan S, Chen H, Li Y (2020) Ferritin in the coronavirus disease 2019 (COVID-19): a systematic review and meta-analysis. *J Clin Lab Anal* 34(10):e23618. <https://doi.org/10.1002/jcla.23618>
 39. Baier MJ, Wagner S, Hupf J, Evert K, Evert M, Sossalla S, Jungbauer C, Maier LS, Neef S, Mustroph J (2022) Cardiac iron overload promotes cardiac injury in patients with severe COVID-19. *Infection* 50(2):547–552. <https://doi.org/10.1007/s15010-021-01722-6>
 40. Chiang SK, Chen SE, Chang LC (2018) A dual role of heme oxygenase-1 in cancer cells. *Int J Mol Sci* 20(1):39. <https://doi.org/10.3390/ijms20010039>
 41. Sharma A, Garcia G Jr, Wang Y, Plummer JT, Morizono K, Arumugaswami V, Svendsen CN (2020) Human iPSC-derived cardiomyocytes are susceptible to SARS-CoV-2 infection. *Cell Rep Med* 1(4):100052. <https://doi.org/10.1016/j.xcr.2020.100052>
 42. Han Y, Zhu J, Yang L, Nilsson-Payant BE, Hurtado R, Lacko LA, Sun X, Gade AR, Higgins CA, Sisso WJ, Dong X, Wang M, Chen Z, Ho DD, Pitt GS, Schwartz RE, tenOever BR, Evans T, Chen S (2022) SARS-CoV-2 infection induces ferroptosis of sinoatrial node pacemaker cells. *Circ Res* 130(7):963–977. <https://doi.org/10.1161/CIRCRESAHA.121.320518>
 43. Dixon SJ, Lemberg KM, Lamprecht MR, Skouta R, Zaitsev EM, Gleason CE, Patel DN, Bauer AJ, Cantley AM, Yang WS, Morrison B 3rd, Stockwell BR (2012) Ferroptosis: an iron-dependent form of nonapoptotic cell death. *Cell* 149(5):1060–1072. <https://doi.org/10.1016/j.cell.2012.03.042>
 44. Vlahakos VD, Marathias KP, Arkadopoulos N, Vlahakos DV (2021) Hyperferritinemia in patients with COVID-19: an opportunity for iron chelation? *Artif Organs* 45(2):163–167. <https://doi.org/10.1111/aor.13812>
 45. Iles L, Pfluger H, Phrommintikul A, Cherayath J, Aksit P, Gupta SN, Kaye DM, Taylor AJ (2008) Evaluation of diffuse myocardial

- fibrosis in heart failure with cardiac magnetic resonance contrast-enhanced T1 mapping. *J Am Coll Cardiol* 52(19):1574–1580. <https://doi.org/10.1016/j.jacc.2008.06.049>
46. Ismail TF, Hsu LY, Greve AM, Gonçalves C, Jabbour A, Gulati A, Hewins B, Mistry N, Wage R, Roughton M, Ferreira PF, Gatehouse P, Firmin D, O'Hanlon R, Pennell DJ, Prasad SK, Arai AE (2014) Coronary microvascular ischemia in hypertrophic cardiomyopathy—a pixel-wise quantitative cardiovascular magnetic resonance perfusion study. *J Cardiovasc Magn Reson* 16(1):49. <https://doi.org/10.1186/s12968-014-0049-1>
47. Tanacli R, Doeblin P, Götze C, Zieschang V, Faragli A, Stehning C, Korosoglou G, Erley J, Weiss J, Berger A, Pröpper F, Steinbeis F, Kühne T, Seidel F, Geisel D, Cannon Walter-Rittel T, Stawowy P, Witzernath M, Klingel K, Van Linthout S, Pieske B, Tschöpe C, Kelle S (2021) COVID-19 vs. classical myocarditis associated myocardial injury evaluated by cardiac magnetic resonance and endomyocardial biopsy. *Front Cardiovasc Med* 8:737257. <https://doi.org/10.3389/fcvm.2021.737257>

Publisher's Note Springer Nature remains neutral with regard to jurisdictional claims in published maps and institutional affiliations.

Springer Nature or its licensor (e.g. a society or other partner) holds exclusive rights to this article under a publishing agreement with the author(s) or other rightsholder(s); author self-archiving of the accepted manuscript version of this article is solely governed by the terms of such publishing agreement and applicable law.